PRELIMINARY RESEARCH AND DEVELOPMENT OF THE CESIUM TUBE ACCURACY EVALUATION SYSTEM

David A. Howe, Howard E. Bell, Helmut Hellwig, and Andrea DeMarchi*

Time and Frequency Division
National Bureau of Standards
Boulder, Colorado 80302 USA

Abstract

A method has been developed which measures the velocity distribution of the atoms in a beam tube using the Ramsey dual interaction region principle. The method involves pulsing the RF excitation signal at a period related to the atoms' time-of-flight between the interaction regions. The pulse method, with its ability to measure velocity distribution enables calculations of cavity phase shift and second-order Doppler effect. This research has motivated the development of a system, complete unto itself, for determining the accuracy of cesium beam tubes. Design goals for the system are outlined. The system development to date is discussed. Frequency synthesis is accomplished at 5.00688 MHz. This avoids frequency synthesis at X-band and thereby eliminates packaging and weight problems. A novel synthesizer design is used which incorporates a digital frequency lock of the 5.00688MHz VCXO. A resolution of 1.4 millihertz/second is realizable; lock is within 2.8×10^{-10} at one second of a 5.0000 MHz reference with potential to better than 1×10^{-12} at one second. This synthesizer and its application to the accuracy evaluation system are discussed. Some results on the evaluation of commercial cesium beam tubes are given.

Introduction

A complete evaluation of accuracy for a cesium beam standard necessitates a precise measurement of the velocity distribution of the atomic beam. From the velocity distribution of a beam tube, one can calculate the frequency offset of the device due to the second-order Doppler effect. The offset due to cavity phase shift may also be inferred from measurements of resonance frequency changes as a function of velocity. The Doppler shift and cavity phase shift are usually the most notable measurements because their effects contribute significantly to the accuracy error budget for a beam tube.

Precise measurement of the velocity distribution yields information about the design of the optics in a beam tube. We can acquire knowledge about the flight of the atoms through the tube and can more accurately judge the effects of mechanical adjustments or environmental influences by noting changes in the distribution. Diagnostic testing of the beam tube and its optical system is more realizable.

The Ramsey-type cesium beam tube employs two separated microwave interaction regions which are part of the same cavity. With a continuous (CW) microwave signal applied to the cavity, all atoms in the beam are subject to an RF excitation field at each interaction region. By modifying the microwave signal so that it is a series of RF bursts of prescribed duration and period, we excite a cluster of atoms which are in the first region at the time of the burst. On the subsequent RF burst, we again excite some atoms in the cluster at the second interaction region. The period between bursts relates directly to the time-of-flight of the atoms between the two regions if the tube is to have a Ramsey spectral line. In practice, we gate the tube's RF excitation at different periods (corresponding to different velocities) and then measure the intensity of the Ramsey pattern. The principle is the same as the mechanical beam chopper used in particle velocity experiments. Figure 1 shows an analogy to determining the velocity of a pellet.

A system was designed and constructed for measuring beam tube velocity distributions. The system relies on the pulse technique for these measures. This manuscript describes the development of the hardware to date. This development has led to interesting research into design techniques used for measuring the intensity of the Ramsey pattern. In particular, digital frequency synthesis of 5.00688 MHz (a submultiple of the desired Cs resonance frequency) is produced from 5.00000 MHz, a common lab reference frequency. Velocity distribution data is presented for some commercial beam tubes and for NBS 4, (primary frequency standard). Effects of measurements with different C-field intensities and Cs oven temperatures are illustrated. Finally, we will look at some future areas of interest which exploit the use of tubes operating in the pulsed mode.

Pulsed Operation of Beam Tubes

The concept of pulsed operation of cesium beam tubes for the measurement of atomic velocities was introduced and analyzed earlier [1]. In the most commonly used Ramsey-type beam tubes, state-selected atoms travel through two RF interaction regions separated by a distance L. For a particular atomic velocity, the hyperfine transition probability due to RF excitation using only the interaction term (Ramsey pattern) due to the coherent action of the two cavity regions is given by [2]:

$$P_{p\to q} = \sin^2 \frac{2b\ell}{v_n} \cos^2 \frac{1}{2}\left[\left(\lambda + \frac{v_n^2}{2c^2}\,\omega_o\right)\frac{L}{v_n} - \delta\right] \quad (1)$$

*On leave from the Instituto Elettrotecnico Nazionale, Torino, Italy.

where: b is the microwave field parameter (proportional to the square root of the microwave power.)

v_n is the atomic velocity

ω_o is the atomic resonance frequency

$\lambda = \omega_o - \omega$(atomic resonance − RF excitation frequency)

δ is the cavity phase shift

The distribution of atomic velocities $\rho(v)$ in most beam tubes is for the most part, determined by the design of beam optics. The mean transition probability close to resonance is given by equation #1 weighted with respect to $\rho(v)$ and integrated over all v_n. If we vary the excitation frequency, $P_{p\ q}$ varies strongly as λ. The expression is at maximum at resonance, i.e., $\lambda = 0$ and other maxima are at $\lambda = \frac{n\ 2\pi\ v_n}{L}$ where n = 1, 2, 3. . . also. The frequency and amplitude associated with other maxima depend on L and ρ (v).

It's possible to make a simple change of variables so that $P_{p\to q}$ is expressed with respect to time. Under CW operation of the tube, atoms are subject to RF excitation at each interaction region for a duration given by:

$$\tau_n = \frac{\ell}{v_n} \qquad (2)$$

The transition probability associated with the interaction regions at resonance is given by the first term of Equation #1:

Interaction region: $$P'_{p\to q} = \sin^2 \frac{2b\ell}{v_n} = \sin^2 2b\tau_n \qquad (3)$$

The combined effect of two interaction regions separated by L yields equation # 1. RF excitation of the atoms at one time (corresponding to the first interaction) and then subsequent coherent excitation at a time T later (at the second interaction region) creates the Ramsey spectral line characteristic. T is related to L for a particular atom by its velocity:

$$T_n = \frac{L}{v_n} \qquad (4)$$

For atoms traveling with velocity v_n, we have

$$P_{p\to q} = \sin^2 2b\tau_n \cos^2 \tfrac{1}{2}\left[\left(\lambda + \frac{v_n^2}{2c^2}\omega_o\right)T_n - \delta\right] \qquad (5)$$

We see that in CW operation of the tube, each atom is excited (pulsed) once for period τ and subsequently excited (pulsed) again at time T later. If we operate the tube so that the RF excitation appears as bursts of duration τ and period T_n. We are able to make the tube operate conventionally for a particular v_n given by equation #4 and illustrated in Figure 2. The transition probability in pulsed operation is shown in equation #5 with τ substituted for τ_n. We want $\sin^2 2b\tau$ to be the same for all velocities of interest. This means τ should be short compared to $\frac{\ell}{v_{max}}$ so that even the fastest atoms have the same transition probability as the slowest in the interaction region. Ramsey spectral line characteristics are produced for both CW and pulsed operation in the pulsed mode, the amplitude of the Ramsey (i.e. peak-to-valley signal intensity) is proportional to the number of atoms at v_n corresponding to a given T_n. The Ramsey spectrum assumes the characteristics of a monovelocity spectrum described by equation #1. Also the maxima at $\lambda = \frac{n\,2\pi v_n}{L}$ are at approximately the same amplitude near the resonance. This is because only one atomic velocity is preferred by the tube, hence the maxima are independent of ρ (v).

We want the tube to operate with only a particular atomic velocity and reject all others. In reality, we have a finite velocity window. The resolution of velocity measurements is limited by the width and shape of the velocity window Δv and it is ultimately given by $\frac{\ell}{L}$ (i.e. the tube design), since $\frac{\Delta v}{v_n}$ can never be any smaller than approximately this regardless of the chosen pulses [1]. For a tube operating in the monovelocity mode we find for the frequency distance of the first valley from ν_o a value specified by :

$$\Delta\nu_n = \frac{v_n}{2L} \qquad (6)$$

where $\Delta\nu_n = \nu_o - \nu_{valley}$ at v_n. We see that in order to measure the intensity of the Ramsey pattern while the tube is operating with atomic velocity v_n, it is necessary to measure with respect to the valley frequency given by $\frac{v_n}{2L}$. Since v_n extends across a range given by ρ (v) then $\Delta\nu_n$ must similarly be variable across a certain range. Furthermore, if a velocity measurement system is to accommodate a variety of tube lengths L, then $\Delta\nu_n$ must extend over quite a large range which is given by ρ(v) and L. In the extremes we want to accommodate velocities from 50m/s to 500 m/s and L values from 0.05 m (small commercial tube) to 5m (longest laboratory tube). This requires a range of $\Delta\nu_n$ from 5Hz to 5000 Hz.

If short pulses ($\tau < \frac{\ell}{v_n}$) are used in order to

have constant transition probability for all velocities in the interaction regions, and at the same time we are dealing with a tube of long length L, then the Ramsey signal may be too small to yield a good measurement. The tube is only operating for time τ (its duty cycle is $\frac{\tau}{T_n}$). In these instances, it is possible to lengthen the pulse width for better signal-to-noise. By lengthening the pulse, we will violate $\tau < \frac{\ell}{v_n}$ and thus the transition probability will no longer be independent of v, as is the case for short pulses. If we make the ratio $\frac{\tau}{T_n}$ = constant for long pulses $\left(\tau > \frac{\ell}{v_n}\right)$ it is possible to adjust the microwave excitation power so that the transition probability is the same for all given v_n. The condition for this is [1]

$$\frac{P_n}{P_o} = \left(\frac{T_o}{T_n}\right)^2 \qquad (7)$$

where P_o is optimum power for some given T_o, and P_n is optimum power for another pulse period T_n corresponding to a selected velocity v_n. We call this technique (i.e. $\tau > \frac{\ell}{v_n}$ for all v_n combined with power adjustment according to equation #7) the long pulse method. It permits the measurement of velocity distributions of long tubes with a good signal to noise ratio.

The complete evaluation system is primarily intended to automate the accuracy evaluation of the NBS frequency standards NBS-4 and NBS-5. The most important limitation in accuracy evaluations of cesium beam tubes are the second-order Doppler effect and the cavity phase shift (2). Both effects depend on the velocity of the atoms in the beam. The second-order Doppler effect is due to the movement of the atoms relative to the interrogating system (cavity, observer at rest). It's magnitude (fractionally) is given by (compare equation #1):

$$\frac{\Delta\nu}{\nu} = -\frac{1}{2}\frac{v_n^2}{c^2}$$

where c is the speed of light. For typical beam tubes, this effect is of the order of parts in 10^{13}. The cavity phase shift comes from a slight difference in the phase between the two interaction retions of the Ramsey cavity due to machining tolerance limitations in manufacturing. The magnitude of the effect is, at best, reducible to small values, but ultimately necessitates measurement. The corresponding frequency shift is given by $\frac{\Delta\nu}{\nu} = \frac{\delta v_n}{2\pi L \nu_o}$ where δ is the cavity phase difference (in radians), and ν_o is the resonance frequency. For beam tubes with very carefully made cavities, this term is typically of the order of parts in 10^{12}.

In order to accurately determine the second-order Doppler effect, some mean squared velocity of the given velocity distribution must be known. High accuracy requires detailed knowledge of this distribution; the greater the detail, the greater the desired accuracy. The velocity measurement system is capable of determining the velocity distribution to a few percent accuracy. Thus the second-order Doppler effect can be determined with similar accuracy, i.e., to better than 1×10^{-14} residual effect on the frequency uncertainty.

In order to determine the phase shift term, a frequency measurement for at least two different velocity settings must be performed. The most traditional method for this is a sign change of ν nominally, i.e., beam reversal [4]. The PTB has employed a switching of the first state selecting magnet from a strong magnet (focussing higher velocities) to a weaker magnet (focussing lower velocities) [5, 6]. Other methods which can be employed are the power shift technique and the pulse technique. In the use of the power shift technique, the mean velocity of the atoms which perform successful transitions is changed by virtue of the dependence of the transition probability on the applied microwave field intensity. Thus, a higher microwave power may lead to a higher mean velocity. A pulsed operation will permit a preselection of velocities through setting of the pulse period. Corresponding frequency measurements yield the cavity phase shift information. At the present time, the determination of the cavity phase shift at NBS, using the power shift or the pulse method, is done in a separate experiment. Following the acquisition of the velocity distribution with the system described in this paper, suitable microwave power settings and/or pulse settings are computed and executed manually. The results are then processed in a computer program which again utilizes the velocity distribution to yield both second-order Doppler and cavity phase shift biases [7].

The planned future complete evaluation system will automatically perform the functions just described and execute the necessary computations on-line.

Hardware

In order to obtain full evaluation, we set out to achieve these basic specifications for the velocity measurement system:

1. The system should be able to measure velocity distributions for tubes with length between regions of L = 5cm to L = 5 meters assuming a velocity range from 50m/s to 500m/sec. The measurement resolution shall equal or excell the inherent accuracy allowed by the pulse technique.

2. The system should be self-contained and portable (needing a 5MHz reference signal). Two connections shall be necessary from the system to a powered Cs beam tube: RF excitation to the cavity and ion current from the detector.

3. The system should acquire data as quickly as possible, automatically, and with minimum preparation and knowledge by an operator.

We have successfully built a system capable of meeting these criteria. Completion of this velocity measurement apparatus represents the first phase in the development of an accuracy evaluation system. Figure 3 is a block diagram of the elements which comprise the velocity measurement system. 5MHz from the laboratory or from the system's local oscillator is used as a reference for two synthesizers. One generates a submultiple of the Cs resonance frequency, and the other produces the same submultiple of the first adjacent Ramsey valley. A multiplier fed alternately by the two synthesizers produces the microwave cavity excitation (9.192... GHz) for the beam tube. The switching between the peak and valley synthesizers is provided by a modulator at a 1 Hz rate. The microwave signal is fed to a power attenuator, then through a pin-diode switch. The signal is gated by the switch which is driven by a pulse generator. At this point, connection is made to the cavity of the powered beam tube. The ion current from the detector in the tube is coupled back into the velocity measurement apparatus. The detector signal is amplified and sent through a low-pass filter. The system's modulation rate is 1Hz so signals above 1Hz are attenuated. The preamp and filter are connected to the demodulator. Demodulation is achieved using a synchronous detector. This output is fed directly to a strip chart recorder. The positive deflection of the pen corresponds to the peak-valley amplitude, i.e., the Ramsey pattern amplitude. A sequencing circuit built into the strip chart recorder actuates a reel-to-reel paper tape reader. As the chart paper advances, the tape reader increments to successive blocks of data. Each block controls the valley synthesizer frequency, the pulse period T_n and width and the power to the beam tube's cavity. These elements control the particular velocity which the tube will select. A paper tape has been programmed which will allow the system to accommodate tubes ranging from L = 5cm to L = 5m. The number of data points in a distribution covering the velocity range of 100 to 300 m/s can be extended to over 100 points. It takes about thirty minutes to prepare the measurement system. This preparation includes tuning the reference, finding the peak atomic velocity of the tube under test, determing the power and pulse width for good signal-to-noise out of the tube, and setting the gain of the detector preamp to handle the levels given by the detector. The total measurement time needed to acquire a velocity distribution, is about one hour. Greater precision may be achieved by averaging each data point for a longer period.

Although the elements comprising the system are uncomplicated, the flexibility of the system must be great in order to accommodate a variety of beam tubes. At the same time, it is necessary to have each element operating with a high degree of stability. In the design of the system, we resorted to digital techniques and the use of integrated circuits as often as possible so that the system would be compact, rugged and reliable.

The pulse generator is a divider chain which counts down a 500kHz time-base oscillator. The amount of division(modulus) is programmed by adjusting the time interval before the divider chain is reset to zero following a prescribed count. This scheme allows setting the pulse period to a precision of $2\mu s$. The availability of low-cost I.C. dividers makes possible as much range in the modulus as we desire simply by making the chain as long as we desire. The reset for the divider chain, hence the modulus, determines the pulse period T_n. The width τ is adjusted by a one-shot. Provision is made for τ to be adjusted by a front panel knob. The pulse generator has a period ranging from $10\mu s$ to 10ms in $2\mu s$ increments. Pulse width ranges from zero to 5ms. The pulses drive a pin diode switch and gate the microwave excitation signal on and off. The microwave power attenuator is also a pin diode. Bias voltage for the diode is derived from a linearizing circuit which makes the attenuation linearly proportional to the control voltage. A D-A converter allows the microwave attenuation to be digitally programmable from the tape reader which is a necessity for the long pulse method. The microwave power to the cavity ranges from $37\mu W$ to 3.75mW (20dB range) in $8.2\mu W$ increments.

The detector preamp is an operational amplifier having low 1/f noise. Its voltage gain is adjustable from unity to 100. The low-pass filter response is adjustable to a small extent, but is principally used to attenuate high frequency noise above 1Hz. The filter is adjusted to pass the peak-to valley modulation rate of the system.

The demodulator is a synchronous detector which responds to an AC signal at only the modulation rate. This is achieved by a synchronous sample-and-hold of the detected "peak" amplitude and sample-and-hold of the detected "valley" amplitude. The output of the demodulator is the difference of the amplitudes. It represents a signal in which the level is proportional to the peak-to-valley amplitude.

Unique elements of the system are the synthesizers used to generate the 5.00688MHz signals which are at submultiples of the peak and adjacent valley at Cs resonance. We wanted to make the Cs excitation signal tunable over a range of about 2kHz.

At the same time, we wanted to know that we were at a prescribed frequency to within ± 1Hz referred to a calibrated 5.00MHz source. With such a microwave signal, it is possible to accommodate a variety of linewidths (recall we must modulate between peak and valley), hence a variety of tube lengths L. Conventional methods call for the 5MHz source to be multiplied to a microwave signal near Cs resonance, and then for power, a klystron is locked to a frequency which is offset by a synthesizer. The synthesizer may then be tuned in order to get a frequency change in the microwave excitation. This method has the advantage that the frequency stability of the synthesizer need not be very high. Frequency fluctuations as high as 5Hz can be tolerated for the narrowest tube line-widths. There are, however, problems associated with this method when one is trying to meet our objectives:

1. The method is bulky requiring several microwave parts in order to achieve efficient lock of the klystron and clean spectrum.

2. Continuous and reliable lock of the klystron depends to a large extent on environmental factors. Immunity to shock and vibration is relatively low.

We chose to eliminate the microwave "plumbing" and multiply directly from a 5.00688 MHz synthesizer to X-band with the last stage of multiplication being a step-recovery diode and tuned cavity. The frequency stability specifications for this synthesizer are quite strict because its frequency (hence its fractional frequency fluctuations) is multiplied by 1,836. For a maximum fluctuation of 5Hz at X-band, we can only tolerate a 2.7 mHz excursion at 5.00688 MHz. In order to design for the capability to lock to this precision, it's necessary to resolve frequency fluctuations to 2.7 mHz or better.

When a 5.00 MHz stable reference is mixed with 5.00688 MHz, the beat frequency is 6.88 kHz. A digital counter with a time-base reference of 5.00MHz can measure 6.88 kHz to a resolution of $\frac{6.88\ \text{kHz}}{5 \times 10^{6}} = 1.38$ mHz in one second. This resolution is the same as that associated with the frequency fluctuations between the 5.00 MHz and 5.00688 MHz since it's the beat note which is being counted. Figure 4-A shows a scheme which uses a time-interval counter to measure the period of the beat. Note that in order to achieve 1.38 mHz resolution in one second, the time interval counter may be entirely digital. A change of one increment in the count corresponds to 1.38 mHz at 5.00688 MHz, or 2.8×10^{-10} / s. The resolution may be increased by allowing the counter to gate with a period longer than one second. It is also possible to increase the resolution by adding analog interpolation with a 5.000 MHz time-base reference, a digital counter can interpolate period measurements to 2×10^{-7} at 1s. This could be extended to 1×10^{-9}/s. by using a nanosecond interpolator. This would yield a resolution of 7μHz at 5 MHz. Using a very low noise mixer and op amp (Schmitt trigger), the resolution could be extended by an order of magnitude, but the noise considerations of these devices become important at this resolution.

In order to keep the 5.00688 MHz oscillator at a constant frequency offset relative to the 5.000 MHz reference, a servo system is used which maintains a constant beat note period. This is shown in Figure 4-B. The time-interval count in parallel binary form is compared with a fixed count prescribed by the data from the paper tape reader. The comparator's outputs indicate whether the two binary numbers are equal or unequal. In the case of an inequality, an up-down counter is forced to count up or down depending on whether the counter number is lower or higher than the prescribed count. The binary count in the up-down counter is parallel fed to a 10-bit digital-to-analog converter. The output of the D-A converter then serves as the error correcting voltage which keeps the 5.00688 MHz oscillator at a given frequency offset relative to the 5.000 MHz reference.

This synthesizer does well for our application. Frequency lock is within 2.5 Hz at x-band. There are two synthesizers in the system. The "peak" synthesizer has a manual control of its frequency offset via thumbwheel switches. The "valley" synthesizer gets its frequency offset data from the paper tape reader. Recall that the valley frequency is offset from Cs resonance by $\frac{1}{T_n}$. Thus, for every value of pulse period T_n, we address a different valley frequency. The frequency range of each synthesizer is determined by the range which its oscillator may be moved by voltage control of the varactor. In this instance, the peak synthesizer has a range of about 200 Hz; the valley synthesizer has a range of about 2 kHz.

Planned later phases of the evaluation system will feature an on-line minicomputer capable of executing not only the velocity distribution acquisition but also the optimum prediction and execution of power shift and pulsed techniques including the computation of the related frequency bias corrections, which then include, of course, also the 2nd order Doppler shift. It appears largely to be a software development problem to expand this computer-centered system to also handle the tasks of magnetic field measurement and time domain stability measurements. Thus, we envision that our expanded system may be capable of automatically executing a full accuracy and time domain stability evaluation of our primary cesium standards. This should increase the frequency of full evaluations, reduce measurement errors, and enhance measurement precision. In short, the full evaluated accuracy of our primary standards would be routinely available.

Since, for the most part, the evaluation system relies only on the presence of Ramsey-type cavity structures, its use is obviously not restricted to primary laboratory standards as was demonstrated earlier in the paper. A full accuracy evaluation of commercial tubes, however, is not as readily possible. First, information on the magnetic field is not as accurately possible in commercial tubes as it is in laboratory devices, which were designed for this task. Second, the evaluation of the cavity phase shift poses problems. Any evaluation of this effect would have to rely on the power shift and/or the pulse technique. Both can easily be executed by the evaluation system. However, the interpretation of the results may pose some difficulties depending on the beam tube design. Beam tubes presently feature dipole optics which deflect the beam according to its velocity. At the output of the dipole magnet we therefore find a spatial distribution of velocities in the deflection plane. Each cavity section has typically rather large openings for the beam and, naturally, electrical losses and asymmetries. This causes a spatial phase-distribution across and along the beam openings. The whole cavity therefore can not be totally and uniquely characterized by one phase-shift value δ. Depending on the particular trajectory of the atom sampling the cavity, the cavity may have apparently different phase differences. This, together with the earlier mentioned spatial velocity distribution of the beam after passing the dipole magnet causes $\delta = \delta_0 + \delta(v)$ in a pulse or power shift experiment. Obviously, in certain cases, a power shift or pulse technique related determination of δ (which in this sense may not be well defined because of $\delta(v)$) may be all but impossible. Since this imprecision in δ will effect the measurements more for small L and wide beams, some commercial beam tubes will be difficult to evaluate in terms of high absolute accuracy. Commercial beam tubes featuring narrow beams; low loss cavities and reasonable values for L can be evaluated. The achievable accuracy will not be as good as in long laboratory devices but may still be of practical interest. Regardless of this accuracy aspect, velocity distribution information can always be obtained and used as information input for an alignment check, performance diagnostic, aging diagnostic, etc. Also, the prediction of microwave power level independent settings is unrestricted, a potentially important aspect discussed later. In view of the importance of narrow beams in order to achieve highest accuracy with regard to the most important accuracy limiting effect, cavity phase shift, serious consideration should be given to hexapole state selecting magnets which appear to lead closest to an ideal beam optics design. Their use (only the primary standard of the Physikalisch - Technisch Bundesanstalt uses them presently) may not only significantly enhance the accuracy of evaluations but also further improve long term (months/years) stabilities because of a more stable beam trajectory in the cavity with regard to spatial phase variations.

Data

In most beam tubes, the oven operates at approximately 90°C. The corresponding most probable velocity is about 240m/s. The fact that all tubes on which we are reporting show peaks in their respective $\rho(v)$ which are at velocities substantially below 240m/s indicates the dominating influence of the beam optics geometry on $\rho(v)$.

The velocity measurement system is able to acquire data points representing the peak-to-valley amplitude of the Ramsey pattern at a specified T_n. The paper tape reader automatically sequences the tape through all its data blocks from a command given by circuitry in the strip-chart recorder. Figure 5 is a strip-chart record of raw data taken by the system of a commercial tube. Recall that T_n, ν_{valley}, and microwave power change each time the paper-tape is advanced. T_n values corresponding to low velocities start at the left of the record; the up direction corresponds to bigger peak-to-valley amplitudes. Note that the amplitude passes through a maximum as the system makes the tube select higher velocities. More to the right, we see a sudden increase in the amplitudes. This is a measure resulting from atoms travelling at 1/3 the values of these velocities. For high velocities, there is a correspondingly high frequency offset associated with the first valley adjacent to the Cs resonance. The frequency of this first valley also is the frequency of the second adjacent valley for atoms travelling at 1/3 the velocity. These lower velocity atoms interact with every third pulse of the pulse train. For most beam tubes, we may expect to encounter at most the first of these aliases as a result of pulse rate being at a harmonic for a lower velocity having a substantial number of atoms. It's a simple matter to subtract out the effect since we know precisely the Ramsey amplitudes associated with atoms up to the first alias.

In order to calculate $\rho(v)$ from the strip-chart record, we must multiply T_n by the values obtained for each v_n. This multiplication equalizes the data points since long pulse periods make the tube operate with a smaller duty cycle than short pulse periods, hence the Ramsey amplitude will necessarily be smaller. Then it is conventional to normalize $\rho(v)$.

We will report the results of velocity measurements on three commercial beam tubes (denoted by A, B, and C) and NBS-4, one of our primary frequency standards. Except where noted, tubes were operating in the pulsed mode as they would be set up to operate in the CW mode. It took about one hour to complete the measurement for each tube. All use offset beam geometry. Excitation power was adjusted for maximum transition probability (eq. 5) corresponding to τ_n for each tube. Each point represented about 40

seconds of averaging. Figure 6 shows the velocity distribution for tube A. For this tube, L = 17.71 cm and $\tau = 10\mu s$. Tube A displayed very good signal-to-noise ratio as is evidenced by the low scatter of data points. The peak of the distribution is at a relatively low velocity which is unique among commercial tubes of this size. Furthermore the distribution is narrow indicating a substantial amount of velocity selection designed into the beam optics.

Figure 7 is a velocity measurement of tube B. In this case, L = 25 cm, $\tau = 43\mu s$. Two distributions are shown; one is with the C-field adjusted to 180mOe. Since it is the case that as τ becomes smaller, the Rabi pedestal becomes broader, we were concerned about the effects of exciting field dependent transitions using short pulses. Increasing the C-field strength showed no appreciable change in the measured velocity. distribution except for a lowering of the low velocity cut-off of $\rho(v)$ at high magnetic fields. The two distributions have ranges of scatter which overlap to a large degree, so it's difficult to assess the effect more exactly. It is necessary to increase the C-field intensity as the pulses become smaller than $\tau_n = \frac{\ell}{v_n}$ in order to minimize any effects due to field dependent transitions.

Figure 8 shows two velocity distributions for tube C; one is with a nominal oven temperature (90° C) and the other is with a high oven temperature (107° C). For this tube, L = 12cm, and $\tau = 13\mu s$. Signal-to-noise ratio was as good as in tube A. With the difference in temperature, we expect an overall change in the velocity distribution of 3% as calculated from a shift in this most probable thermal velocity. The measured distributions did, in fact, show this change. It indicated to us that the measurement resolution was at least 3% for tube C. The peak of the distribution is at a relatively high velocity and the distribution is broad. This is a characteristic of many commercial tubes. High velocity attenuation is not as predominant. The rise at high velocities is due to the slower atoms interacting with every third pulse of the pulse train as described earlier.

Figure 9 is the velocity distribution measured for NBS-4, with L = 52.36 cm and $\tau_n = 50\mu s$. We see that there is an observably smaller number of atoms travelling at $v_n = 190 m/s$. The beam optics of NBS-4 contain stops which suppress velocities in a narrow range slightly greater than the peak velocity. The optics configuration causes the beam to split into two beams, one being a higher velocity trajectory than the other. The type of velocity distribution shown in Figure 8 is one usually associated with on-axis configurations, although NBS-4 uses offset geometry. [8]

In Figure 10 the linear mean velocity of beam tube A is plotted as a function of microwave power, i.e. the term $b\ell$ (see eq. 1). This plot was obtained from Figure 6 by calculation. The plot shows that the mean velocity increases from the optimum power value by about 40% until it peaks at approximately 4.8dB above optimum power. A velocity minimum is reached at about 8dB above optimum power and a second, lower maximum at +10.8dB.

Neglecting all other velocity dependent frequency shifts, the cavity phase shift term causes a frequency shift which is proportional to this mean velocity. With a non-zero δ (as must be always assumed), the frequency of the tube should vary as the velocity. The measured "power shifted" frequency values, are depicted also in Figure 10 (triangles) using a new ordinate with zero arbitrarily assigned to the P_{opt} value. We notice that the frequency shift indeed follows the pattern of oscillation of the mean velocity, though full quantitative agreement is not obtained. This lack of quantitative agreement probably reflects the degree to which $\delta v \neq 0$.

Figure 10 nevertheless illustrates our capability to predict - using just the velocity distribution information - powersettings where the frequency of the tube is in first order power independent: +4.8dB, +8dB, +10.8dB above opt. power. The operation of the tube at such settings may give some long term stability advantage and may also lower the flicker "floor" of a given device. We have some reason to believe that in the conventional operation of a standard at $P = P_{opt}$, microwave power fluctuations and or drifts may be one cause for the flicker "floor" and long term instabilities. No good data exist presently to support this hypothesis; however, we plan to investigate these aspects experimentally. The sacrifice in short-term stability because of a setting at +4.8dB as compared to optimum power is typically a factor between one and two. This appears a tolerable sacrifice, if the long term stability of existing tubes can be markedly improved.

Conclusion

We have completed the first phase of the cesium tube accuracy evaluation system. We have built equipment which will automatically measure the atomic velocity distribution. It has been shown that the pulse technique is a viable scheme for acquiring a tube's velocity distribution. The equipment has been designed for portability and ease of data acquisition. Measurements may be taken on tubes having a variety of lengths. Additionally we have incorporated a design which will allow other modes such as power shift and time domain stability measurements. We have also incorporated methods for digitally sending or recieving information in each element of the system so that a computer may be interfaced.

The next step in the development of the system will be the incorporation of a minicomputer to perform reduction of new data and analysis of results. For automation the minicomputer will enhance system flexibility and ease of operation. Future prospects call for the full evaluation system to perform a check of a lab standard on a routine basis. In a further advanced mode of operation it may be possible that the minicomputer could be inter-connected in such a way that mechanical and/or electronic corrections could be made to the tube so that the standard would be continuously readjusted to the highest accuracy.

Acknowledgements

The authors wish to thank Dave Glaze and Steve Jarvis for assistance in the data interpretation.

References

[1] Hellwig, H, Jarvis, S, Glaze, D.J., Halford, D., Bell, H.E.: Proc. 27th Annual Freq. Contr. Symp., Ft. Monmouth, pp. 357-366, (1973).

[2] Ramsey, N.F.: Molecular Beams, Oxford University Press, London, (1956).

[3] Glaze, D.J.: IEEE Transactions on I and M, Vol. IM-19, No. 3, August 1970.

[4] Mungall, A.G., Bailey, R., Daams, H., Morris, D., Costain, C.C., Metrologia, Vol. 9, No. 3, pp. 113-127, (1973).

[5] Becker, G., Fischer, B., Kramer, G., Muller, E.K., Mitteilungen, Vol. 69, No. 2, pp. 77-80 (1969).

[6] Becker G.: Mitteilungen, Vol. 83, No. 5, pp. 319-326, (1973).

[7] Jarvis, S.: to be published in Metrologia, July 1974.

[8] Glaze, D.J.: Private communications, May 1974.

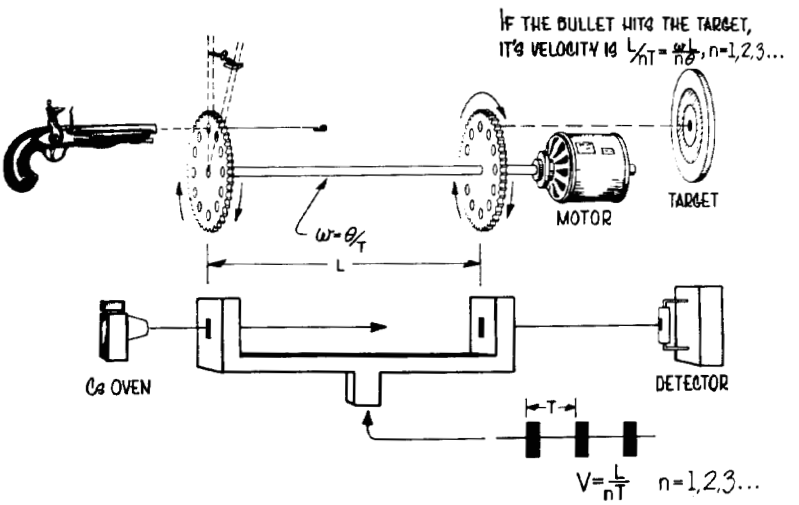

Figure 1: The Ramsey dual-interaction region design allows velocity selection of the atomic beam.

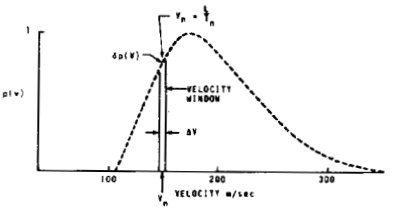

Figure 2: The system makes the beam tube operate for a narrow range of velocities.

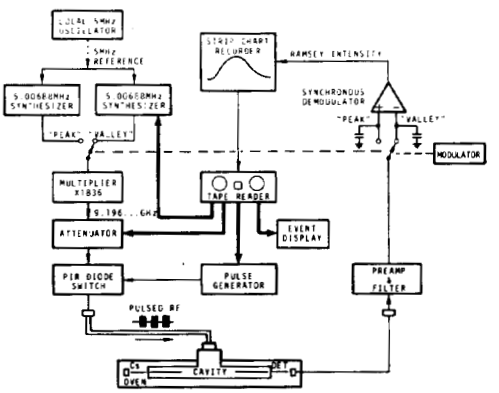

Figure 3: Block diagram of velocity measurement system.

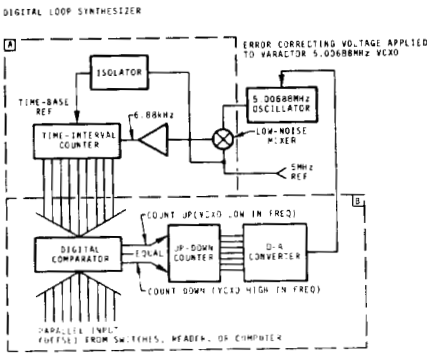

Figure 4: Block diagram of digital synthesizer showing (A) beat frequency period counter and (B) comparator and up-down counter.

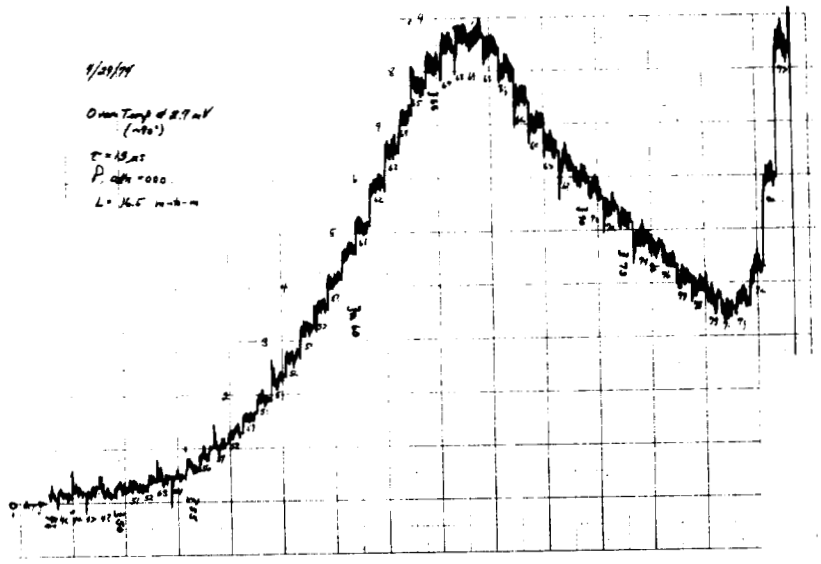

Figure 5: Raw data as produced by the system. It takes about one hour for the complete distribution.

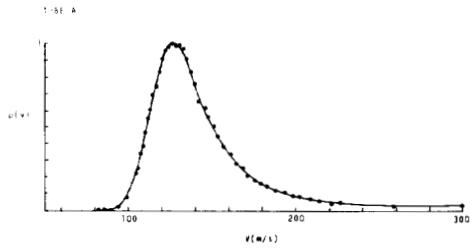

Figure 6: Velocity distribution of Tube A.
L = 17.71cm, τ_n = 10μs

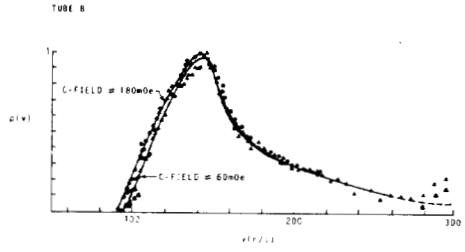

Figure 7: Velocity distribution of Tube B.
L = 25cm, τ_n = 43μs.

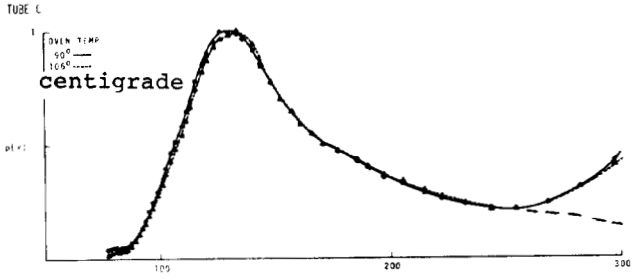

Figure 8: Velocity distribution of Tube C
L = 12 cm, τ = 13μs

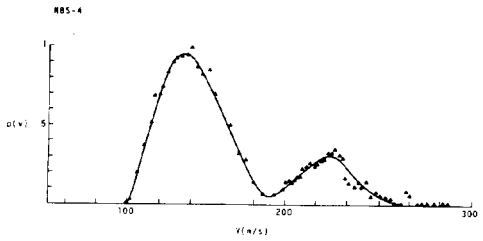

Figure 9: Velocity distribution of NBS-4. L = 52.36cm, $\tau_n = 50\,\mu s$.

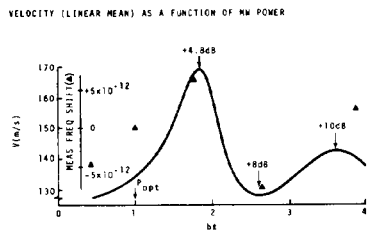

Figure 10: Linear mean velocity of Tube A as a function of microwave power.